The antiviral effects of acteoside and the underlying IFN-γ-inducing action

Song, Xun; He, Jiang; Xu, Hong; Hu, Xiao-Peng; Wu, Xu-Li; Wu, Hai-Qiang; Liu, Li-Zhong; Liao, Cheng-Hui; Zeng, Yong; Li, Yan; Hao, Yue; Xu, Chen-Shu; Fan, Long; Zhang, Jian; Zhang, Hong-Jie; He, Zhen-Dan

Published in:
Food and Function

DOI:
10.1039/c6fo00335d

Published: 01/07/2016

Document Version:
Peer reviewed version

The antiviral effects of acteoside and the underlying IFN-γ-inducing action

Xun Song [a,b†], Jiang He [a†], Hong Xu [a†], Xiao-Peng Hu [a], Xu-Li Wu [a], Hai-Qiang Wu [a], Li-Zhong Liu [a], Cheng-Hui Liao [a], Yong Zeng [c], Yan Li [c], Yue Hao [a], Chen-Shu Xu [a], Long Fan [a], Jian Zhang [a *], Hong-Jie Zhang [b *] and Zhen-Dan He [a *]

[a] Department of Pharmacy, Shenzhen Key Laboratory of Novel Natural Health Care Products, Innovation Platform for Natural small molecule Drugs, Engineering Laboratory of Shenzhen Natural small molecule Innovative Drugs, School of Medicine, College of Life Science, Shenzhen University, Shenzhen 518060, P. R. China;

[b] School of Chinese Medicine, Hong Kong Baptist University, Hong Kong SAR, P. R. China;

[c] The First Affiliated Hospital of Kunming Medical University, Kunming 650032, P. R. China;

[†]Author contributions: Xun Song, Jiang He and Hong Xu contributed equally to this work with the first author.

* **Correspondence:**

Zhendan He (hezhendan@126.com); Hongjie Zhang (zhanghj@hkbu.edu.hk); Jian Zhang (jzhanghappy@szu.edu.cn).

Abstract

There are many herbal teas that are found in nature that may be effective on treating the symptoms and also shortening the duration of the virus infection. When combating viral infections, T lymphocytes are an indispensable part of the human acquired immunity. However, studies on the use of natural products in stimulating lymphocyte-mediated interferon-gamma (IFN-γ) production are very limited. In this study, we found that acteoside, a natural phenylpropanoid glycoside from Kuding Tea, enhanced IFN-γ production in mouse lymphocytes in a dose-dependent manner, particularly in the CD4+ and CD8+ subsets of T lymphocytes. To this end, we suggest that the antiviral activity of acteoside was highly correlated to its inducing ability of IFN-γ production. Mechanistically, the activation of T-bet enhanced the promoter of IFN-γ and subsequently resulted in an increased IFN-γ production in T cells. Collectively, we have found a natural product with the capacity to selectively enhance mouse T cell IFN-γ production. Given the role of IFN-γ in immune system, further studies to clarify the role of acteoside in inducing IFN-γ and prevention of viral infection are needed.

Key words: acteoside, antiviral agent, IFN-γ, immune system, lymphocytes

1 Introduction

The adaptive immune system is remarkable in eliciting specific immune responses against foreign antigens, which mainly are carried out by the T lymphocytes (or T cells), B cells and natural killer (NK) cells.[1] Both T cells and NK cells secrete interferon-gamma (IFN-γ) and promote cell-mediated immune responses.[2] Indeed, IFN-γ plays an important role in the activation of both innate and adaptive immunity system in humans. Nevertheless, IFN-γ is particularly crucial to the antiviral mechanism. [3, 4]

Exogenous recombinant IFNs have been used in various antiviral immunotherapy trials; however, the outcomes were disappointing owing to significant toxicity.[5, 6] Conversely, agents with enhancing ability on IFN-γ production such as recombinant IL-2, IL-12, IL-15, IL-18 and IL-21 when administered individually or in combinations did not provide any satisfactory results either in preclinical and clinical studies.[7-9] These therapeutic approaches failed due to many reasons.[10] For instance, IL-2 exhibited significant infusional toxicities and pro-survival effect on chronic lymphocytic leukemia cells.[11] Patients received high-dose IL-2 therapy were reported with increased risk for renal carcinoma, worsening of diabetic condition and development of myasthenia gravis and polymyositis.[12] The use of recombinant IL-12 and IL-2

also showed systemic toxicity in early clinical trials; these results appeared to be a major obstacle to the clinical application of these ILs.[13, 14]

There are multiple signaling factors involved in the regulation of IFN-γ gene expression and secretion, such as the activation of the mitogen-activated protein kinase (MAPK) signaling pathway and the transcription factor T-bet.[15] The activation of the MAPK pathway is often associated with the ERK phosphorylation cascade in triggering the production of IFN-γ.[15] The activation of the transcription factor T-bet may be critical for achieving a maximal transcription of IFN-γ.

Many viral infections give rise to a great danger to humans and often cause deaths and significant economic loss. In the past decades, influenza viruses that spread around the world in seasonal epidemics resulted in approximately three to five million yearly cases of severe illness and 250,000 to 500,000 yearly deaths.[16] The “Spanish" influenza pandemic caused by the deadly H1N1 virus in the early 20th century killed about 50 million people.[17, 18] At the beginning of the 21st century, the severe acute respiratory syndrome (SARS) outbreak in Hong Kong and mainland China in 2003 affected more than 8000 patients and eventually caused 774 deaths in 26 countries.[19] Moreover, new and re-emerging infectious viral diseases may pose a rising

global health threat, and the risk of spreading these viruses among continents and countries is high. For instance, the recent 2009 H1N1 influenza pandemic was a prime example of emerging infectious disease in the modern world.[20]

A number of preventive and therapeutic measures, including biosecurity, vaccination and antiviral drugs, are routinely used to prevent and treat viral diseases. Vaccines are considered as the basis for the principal prevention of many viral infections, but there are substantial drawbacks.[21] Among the influenza virus genera, vaccination failures have been widely documented, and in the elderly population, in which most of the mortality occurs, vaccines are only approximately 50% effective.[22] In the eventuality of a pandemic infection with a new strain, antiviral drugs represent the first line of defense.[23] Nevertheless, due to their metabolic properties, viruses are difficult to control. As a result, there are yet relatively few effective drugs for the treatment of viral diseases. On the other hand, some highly active antiviral drugs have been reported with adverse effects and complications of the central nervous system and gastrointestinal tract. The rapid emergence of antiviral resistance also limited the usefulness of antiviral drugs.[24, 25] Therefore, novel and effective strategies are urgently sought to overcome the economic and human health risks associated with viral diseases. The exposure of T lymphocytes to some

small-molecule natural products has been shown to increase T-cell proliferative capacity, cytokine production and antiviral activity.[26]

In fact, small-molecule natural products have been the most productive source for the development of drugs. By 2010, about 41% of all new drugs were either natural products or their derivatives.[27] Natural products provide enormous structural diversity, and represent an excellent source for new drug discovery.[28]

In this study, we evaluated a large number of natural products for their ability in enhancing production of IFN-γ in lymphocytes. We discovered that acteoside, a small-molecule phenylpropanoid glycoside obtained from the leaves of *Ligustrum purpurascens* Y. C. Yang (Oleaceae), significantly induced T cell-mediated IFN-γ production. *Ligustrum purpurascens* is traditionally named as "Kuding Tea", a kind of functional tea in China for about two thousand years, which has been reported with antiviral effect.[29] The increased T cell activity was associated with an enhanced T-bet transcription and an up-regulated ERK signaling.[30, 31] Interestingly, NK cell-mediated IFN-γ production was unaffected by the application of acteoside and cytotoxicity of lymphocytes was not observed. Due to the key functions in innate and adaptive immune responses, endogenous IFN- γ has become a focus of study in the research and

immune therapy. We found that only CD4+ and CD8+T cells in the splenocytes were activated by acteoside *in vitro* to produce this effector cytokine, without producing other cytokines such as ILs and TNFs. The selectivity and specificity of acteoside on immune activation should make it the most suitable candidate for developing into a new clinically useful immune modulator.

2 Materials and Methods

2.1 Virus strains

Mouse-adapted influenza virus (A/FM/1/47 H1N1, FM1) was kindly donated by the Institute of Tropical Medicine, Guangzhou University of Chinese Medicine. The virus was amplified in allantoic cavity of embryonated eggs for 48 h at 36°C, and then stored at -80°C. All tests were performed in class II biosafety safety cabinets.

Vesicular stomatitis virus (VSV) NJ strain was kindly donated by the Shenzhen Institute of Tsinghua University, and was propagated and titered by plaque assay on WISH cells.

2.2 Mice

C57BL/6 and Balb/c mice were purchased from Guandong Medical Laboratory Animal Center (Guandong, China). All mice were housed under specific pathogen-free conditions. All animal experiments were performed in compliance with the institutional animal care guidelines and approved by the Experimental Animal Ethical Committee of Shenzhen University Health Science Center, China [Approval number: SYXK (Yue) 2014-0140].

2.3 Isolation of subtype-specific T lymphocytes

Mouse lymphocytes were freshly isolated from the spleen of Balb/c mice using commercial isolation kits (Cedarlane, Canada) according to the manufacturer's instruction. The isolated lymphocytes were freed from NK and B cells, and the purity of lymphocytes was assessed by flow cytometric analysis after staining with CD3-FITC antibody (BD Biosciences, USA). The enriched T cells were further purified with CD4+ and CD8+ magnetic beads and LS columns (Miltenyi Biotec, Germany). The purity of the magnetic bead-purified cells was determined as >99.0% by means of flow cytometric analysis.

2.4 Enzyme-linked immunosorbent assay (ELISA)

IFN-γ level in the cell culture supernatant was determined using a commercial ELISA kit (eBioscience, USA) following the manufacturer's instructions.

2.5 Real-time quantitative polymerase chain reaction (RT-PCR)

Total RNA was extracted from lymphocytes with TRIzol reagent and reversely transcribed to cDNA using a BioRT reverse transcription kit (Biort, USA). Real-time qPCR was performed using SYBR Green Master Mix (Thermo, USA) according to the manufacturer's instructions. A RT quality control and a PCR negative control were included, and β-actin was used as an internal control. Relative gene expression levels were calculated according to the cycle threshold (Ct) values of target genes relative to the internal control gene. The primer sequences are shown in Supporting Information Table 1.

2.6 Cell viability assay

Mouse primary lymphocytes were plated in 96-well plates at a density of 1×10^4 cells and cultured in normal condition. 24, 48 and 72 hours (h) after treatment with various concentrations of acteoside (1.25-160 μM), 10 μL of Cell Counting Kit 8 (CCK-8) (Dojindo Company, Japan) reagent was added to

each well followed by a 3-h incubation at 37°C. Absorbance was measured at 450 nm using a microplate reader (BioTek, USA). Each experiment was performed in triplicate and repeated at least three times.

2.7 Flow cytometric analysis

The apoptotic rates of lymphocytes were determined by flow cytometric analysis using an Annexin V-FITC Apoptosis kit. Briefly, lymphocytes (1×10^6) were seeded in 6-well plates overnight and then treated with various concentrations of acteoside for 24 h. Cells were then harvested by centrifugation (100 × g, 5 min) and washed twice with cold PBS. The staining procedure was performed according to the instructions of the manufacturer (KeyGene, Netherlands) and then the cells were analyzed using a FACScan flow cytometer (Becton-Dickinson, USA). At least three independent experiments were performed.

2.8 Intracellular staining

The assay for intracellular protein detection was performed utilizing the GolgiPlug kit (BD Biosciences) according to a previous reported protocol.[29]

2.9 Western blot analysis

Lymphocytes were seeded in the culture flasks at a density of 1×10^8 cells per well. After treatment, cells were harvested and lysed using ice-cold lysis buffer [20 mM Tris, pH 7.5, 150 mM NaCl, 10 mM EDTA, 1% (v/v) NP-40, 20 mM sodium fluoride, 5 mM sodium pyrophosphate, 1 mM sodium vanadate, 10% (v/v) glycerol, protease inhibitors] and cleared by centrifugation at 20,000 × g for 20 min at 4°C. Protein concentrations were determined by Bio-Rad Protein Assay, and equal amount of protein (50 μg) was electrophoresed on SDS-polyacrylamide gels and transferred onto PVDF membrane. Membranes were blocked with 5% BSA in Tris-buffered saline with Tween-20 (150 mM NaCl, 10 mM Tris-HCl, pH 7.5, 0.1% Tween-20) before probing with appropriate primary antibodies. Subsequently, the membranes were incubated with the corresponding secondary antibodies for 1 h. Protein bands were detected by enhanced ECL reagent (Thermo Scientific, USA), and visualized on Kodak films (Kodak, USA). Scanned images were quantified using the Bio-rad gray image analysis software.

2.10 Reporter assays

About 2.5 kilobases of the IFN-γ translation start site (TSS) were PCR amplified, sequence-verified, and cloned upstream of the firefly luciferase gene in the pGL3-basic reporter vector (Promega, USA). Truncations (5') were generated by restriction digestion using conventional methods. Sixteen hours prior to transfection, RAW264.7 cells were plated at a density of 2×10^4 in full RPMI 1640 culture medium. Immediately prior to transfection, serum-free RPMI 1640 medium was used. Reporter-construct DNA was mixed with Opti-MEM and Lipofectamine and applied to the cells. Six hours after transfection, the medium was replaced with fresh RPMI 1640 supplemented with 10% FBS; 18 h thereafter, acteoside was added at a final concentration of 80 μM. Firefly luciferase activity was measured using the Dual-luciferase reporter assay kit (Promega, USA) at the indicated time points. The Renilla luciferase-containing pGL3-basic vector was used for normalization, and the pGL3-basic vector containing a CMV promoter-driven firefly luciferase gene was included as a positive control. All media and transfection reagents were obtained from Invitrogen (Thermo Scientific, USA).

2.11 Microarray experiments and data analysis

CD3+ T cells were sorted from primary lymphocytes and treated with or without acteoside (80 μM). RNA was extracted from the CD3+ T cells using Trizol reagent (Invitrogen) according to the manufacturer's instructions. Total RNA yield and quality were assessed by using the Agilent 2100 Bioanalyzer. The obtained RNA samples were then subjected to GeneChip Mouse Genome 430 2.0 Array (Affymetrix). The significant differences between samples were analysed by using Robust Multichip Analysis. Each array was normalized for signal intensities across the whole array and locally, using Lowess normalization. From the cDNA array results, genes with absolute fold change greater than two were considered a significant attenuation or stimulation by acteoside. Then, a heat map were constructed using Microsoft Excel and MultiExperiment Viewer.[32]

2.12 Antiviral activity assay *in vitro*

Antiviral activity for IFN-γ was assayed on WISH cells by the dye uptake using VSV as a challenge virus method. Briefly, confluent monolayers of WISH cells in 96-well tissue culture plates were exposed to recombinant human IFN-α2b, the supernatants and acteoside. Twenty-four hours later, the monolayers were washed once with warm medium and then challenged with

100 μL VSV (100 CCID50) per well. After another continuous culture of 24 h, the supernatant was discarded, and the plates were stained with 50 μL neutral red dye. The dye taken up by interferon protected cells was extracted with a solution containing 50% absolute ethanol, 45% distilled water and 1% glacial acetic acid and quantitated spectrophotometrically at 570 nm. All titers are expressed as International reference units (IU). Reference standard was purchased from China Pharmaceutical Biological Products Analysis Institute.

2.13 Antiviral activity *in vivo*

C57BL/6 mice were anesthetized with diethylether. Mice were infected with mouse-adapted H1N1 virus (FM1; 5LD50 intranasal, 25 μl/nare). Infected mice were divided into 4 groups for treatment (n=12 mice for the tests): acteoside (80 mg/kg) and positive drug (ribavirin, 100 mg/kg). The mice were intraperitoneally administrated respectively. The remaining 2 groups (control and infected mice) received equivalent amounts of saline. Lung was collected separately for the histopathology study.

2.14 Lung index

The lungs were isolated and weighed to determine the lung index (a non-direct index of pulmonary edema), defined as follows: lung index=wet weight (g) / body weight (g) ×100%. [33]

2.15 Histopathology

General histological appearance of lung tissue was assessed after routine hematoxylin and eosin (H&E) staining. Briefly, lungs were drop-fixed in 4% paraformaldehyde and then embedded in paraffin. Fixed sections (8 μm) of paraffin-embedded lungs were stained with H&E. Slides were randomized, read blindly, and examined microscopically for tissue damage necrosis, apoptosis and inflammatory cellular infiltration.[33]

2.16 Statistical analysis

An unpaired Student t-test was used to compare two independent conditions (such as acteoside versus control) for continuous endpoints. One-way ANOVA was used for multiple comparisons. The *p* values were adjusted for multiple comparisons using Bonferroni method. All tests are two-sided. A p value < 0.05 was considered statistically significant.

3 Results

3.1 Acteoside selectively enhanced IFN-γ production *in vitro*

Our group has been determinedly screening for potential compounds isolated from medicinal plants with desired immunity-enhancing property.[34, 35] Lately, we found that a phenylpropanoid glycoside, acteoside (Supporting Information Figure 1), isolated from the leaves of *Ligustrum purpurascens* from Yunnan, China, was able to enhance IFN-γ production in mouse lymphocytes. However, no production of IL-2, IFN-α and IFN-β were found after treated with acteoside in lymphocytes in our previous work. We were the first to report that acteoside significantly induced IFN-γ production in primary mouse lymphocytes in a time- and dose-dependent manner (Fig. 1A and B). The maximum production of IFN-γ was obtained 24 h post incubation with acteoside and 80 μM was found to be the optimal dose. The time-course study suggests that acteoside induced IFN-γ expression in lymphocytes in a relatively fast fashion, as soon as 12 h upon treatment (Fig. 1B). Increased IFN-γ mRNA transcription in the primary lymphocytes was assessed by means of RT-PCR (Fig. 1C).

3.2 Cell viability and Apoptosis assay

303 Cytotoxicity of acteoside in primary lymphocytes was evaluated by means
304 of CCK-8 assay. Our result demonstrated that acteoside (1.25 μM to 160 μM)
305 did not induce cytotoxicity when compared with the negative control group.
306 Interestingly, treatment with 80 μM acteoside led to the greatest rate of cell
307 proliferation (Fig. 1D). Thereafter, 80 μM acteoside was selected to be used in
308 the subsequent experiments. To test whether acteoside induced apoptosis,
309 primary lymphocytes were analyzed by a flow cytometric assay with double
310 staining of PI and annexin V-FITC. No significant increase of apoptosis (both
311 early and late apoptotic events) was detected in the acteoside-treated
312 lymphocytes (Fig. 1E and F). At the same time, we studied the intrinsic
313 pathway components, particularly, of the expression of BCL-2 which can
314 regulate the apoptosis of lymphocytes.[36] By means of flow cytometry, no
315 significance difference of BCL-2 expression was observed after treatment with
316 80 μM acteoside in CD4+ and CD8+ T cells (Fig. 1G).
317
318 **3.3 Effect of acteoside on cytokines and surface markers of mouse IFN-γ**
319 **secreting cells**
320 Apart from B cell, T lymphocyte is the major cell type which has been
321 reported to produce IFN-γ. In our study, we found that IFN-γ secretion from

CD3+ T cells was enhanced upon acteoside stimulation when compared to treatment with vehicle control (Fig. 2). From the flow cytometric analysis, we observed that the percentage of IFN-γ+ CD3+ T cells was 26.6% when the primary lymphocytes were treated with 80 μM acteoside. When they were treated with vehicle, the percentage of IFN-γ+ CD3+ T cells was merely 2.53%. However, the percentage of IFN-γ+ cells in acteoside-treated primary CD56+ NK cells and CD19+ B cells did not significantly differ from those subjected to the vehicle treatment (Fig. 2). To investigate whether the acteoside-induced IFN-γ production was T cell subtype specific, we purified CD4+ and CD8+ T cells (purity >99.0%) via FACS for further biochemical assays. The levels of IFN-γ secretion from the purified cells were measured using ELISA. Interestingly, acteoside induced CD4+ and CD8+ cell secretion of IFN-γ (Fig.3 A - D).

3.4 T-bet activated by acteoside

T-bet is a master regulator of IFN-γ gene expression in NK and T cells in mammals, particularly rodents.[37] The induced IFN-γ production occurs mainly through the activation of the JAK-STATs, T-BET, MAPK, or NF-kB signaling pathways.[15] Transcription factors of these signaling pathways are associated

with corresponding binding sites of the regulatory elements of the IFN-γ gene, subsequently enhancing the mRNA synthesis of IFN-γ.[15] Given the critical role of IFN-γ in cell-mediated immunity, it is interesting to study whether the treatment of acteoside affects the expression level of T-bet. Upon the stimulation with 80 μM acteoside, rapid induction of both IFN-γ and T-bet was observed in lymphocytes (Fig. 3). Twenty four hours after acteoside treatment, elevated protein levels of both IFN-γ and T-bet were observed on immunoblots (Fig. 3I), suggesting that acteoside plays a role in regulating the expression level of T-bet. When T cells were sorted into CD4+ or CD8+ cells by FACS, we observed that the treatment of 80 μM acteoside turned 23% of the CD4+ cells and 16.7% CD8+ cells into IFN-γ producers.

3.5 Acteoside activated the ERK pathway in lymphocytes

MAPK pathways are known to play important roles in the regulation of cell survival and proliferation. However, it remains unclear whether acteoside-induced cell proliferation and IFN-γ secretion was associated with modulations of the MAPK pathways. It is speculated that activating the MAP kinase pathways during acteoside exposure and result in cell proliferation. By means

of CCK-8 assay, we showed that proliferation of mouse primary lymphocyte was significantly induced in the presence of acteoside (Fig. 4A).

Further, we found that ERK phosphorylation in primary lymphocytes was increased upon the stimulation of acteoside whereas the level of total ERK was unaffected. As shown in Figure 4B and C, the level of phosphorylated ERK, which represented the active form of ERK, was significantly increased in the group treated with acteoside for 24 h when compared to the control group ($p < 0.01$). Administration of the vehicle had no effect on the level of phosphorylated ERK. When the primary lymphocytes were treated with acteoside at 40 μM, 80 μM and 160 μM for 24 h in the presence of ERK inhibitor U0126, the stimulatory effect on cell proliferation was diminished (Fig. 4D). The Western blot results also demonstrated that the acteoside-induced ERK phosphorylation was reversed by the presence of ERK inhibitor (Fig. 4E and F).

3.6 Acteoside augmented the binding of transcription factor to the IFN-γ promoter in RAW264.7 cells

To test whether the induction of IFN-γ expression by acteoside occurs at the transcriptional level, we transfected an IFN-γ promoter into RAW264.7

cells followed by the treatment with acteoside. With the CMV-Vector serving as a normalizing control, the IFN-γ promoter-driven luciferase activity was assessed in transfected cell lysates after a 24-hour incubation of acteoside. Typically, a 3-fold activation was observed from the transfection of the full-length construct in the presence of acteoside (Fig. 5). The data suggested the mechanism of acteoside-induced synthesis of IFN-γ was regulated at the transcriptional level. The map of the IFN-γ upstream promoter (Mus musculus, GenBank accession no. NC_000076.6) was provided in Supporting Information Figure 3).

3.7 Expression arrays and pathway analysis of acetoside target genes

A hierarchical cluster analysis was provided in Figure 6 for an overview of genes affected by the treatment of acteoside. From the results, we found that among the 973 genes, 49 were significantly affected by acteoside in a positive or negative fashion (Fig. 6). Within these 49 genes, some are responsible for cell growth arrest, DNA damage repairing and apoptosis, including Gadd45, gip1 and Prkar2b. Nevertheless, most of the affected genes are IFN-γ-related transcriptors or T-cell receptor, such as Jak3, Cd3d, Nr4a1 and Sic2a1. To identify the biological pathways associated with the acteoside-induced IFN-γ

secretion, we mapped the target genes of differentially expressed miRNAs to canonical signaling pathways in the Kyoto Encyclopedia of Genes and Genomes (KEGG). The results showed that 23 statistically remarkable categories ($p < 0.05$) were enriched (Table 1). As shown in Table 1, the enriched genes were found to be involved in immune-related pathways, such as the Jak-STAT signaling pathway, NK cell-mediated cytotoxicity and cytokine-cytokine receptor interactions. Taken together, these results further strengthened the effect of acteoside was largely associated with the regulation of endogenous IFN-γ.

3.8 The antiviral activity of acteoside

When purified primary mouse lymphocytes (1×10^7 cells/ml) were treated with acteoside at 20, 40, 80, and 160 μM for 48 h, we found that IFN-γ levels in the supernatants were concentration dependently increased to 2821.06 pg/ml, 3025.00 pg/ml, 3354.70 pg/ml and 3392.27 pg/ml respectively, $p < 0.001$ when compared to the control culture. ConA was used as a positive stimulant in this experiment and it significantly increased the IFN-γ production ($p < 0.001$) when compared to the control culture (Fig.7A). In the antiviral assay, pretreatment with acteoside at different concentrations produced no antiviral

activity and was comparable to the control culture (Fig.7B). Pretreatment with supernatants from lymphocyte cultures under 80 μM and 160 μM acteoside showed significant antiviral activities.

Under microscopic examination, we found that the VSV infection resulted in the formation of cytopathic effect (CPE) 24 h post infection. As the virus replicates, the infected cells round up and detach from the cell culture plate. The first panel showed the uninfected WISH cells whilst and the other panels showed the infected cells with different treatments (Fig.7C-E). Different levels of CPE in WISH cells infected with VSV were observed upon different treatments. WISH cells pretreated with supernatants from acteoside group resulted in a lower percentage of infected cells when compared to the control group. While, the group treated with acteoside alone also showed severe cell damage. It indicated that the WISH cells which pretreated by the supernatant of acteoside could be protected from the infection of VSV. These suggest that IFN-γ, induced by acteoside, may be of clinical significance in host defense mechanisms against various infections.

3.9 Effect of acteoside on histopathology of lungs

Histologically, mouse-adapted H1N1 virus (FM1)-infected animals showed typical lesions of influenza A virus infection as reflected by significant inflammatory changes in the lungs, exudation of alveoli, histolytic alveolitis and lung consolidation. The weight ratio of lung to body of the acteoside group mice was markedly decreased when compared with the H1N1-infected group ($p < 0.05$; Fig. 8A and B). Control mice showed no lesions in lungs (Fig. 8). To be more specific, pulmonary sections of the control mice showed visible bronchi with ciliated columnar epithelia, as well as clear alveolar sac structures and small arteries. No fiber proliferation or bubble wall thickness was observed (Fig.8a). The H1N1-infected mice showed severe infiltration of inflammatory cells clustered around the bronchioles, increased exudation in alveoli, and consolidation of the lungs (Fig. 8b). Ribavirin treatment presented slight infiltration of inflammatory cells clustered around bronchioles and partial consolidation of the lung (Fig. 8c). Pathological changes in the lungs of acteoside-treated mice were minor when compared to the H1N1-infected mice received no treatment (Fig. 8d). The acteoside treatment group (80 mg/kg) showed fewer inflammatory signs in the alveolar region; merely some local bubble wall thickening and some congestion in broken blood vessels were

observed. We suggest that acteoside ameliorated lung lesions in mice with acute respiratory distress syndrome.

4 Discussion

Lymphocytes are important immune cells with a capacity to regulate immune responses including the destruction of tumor cells and clearance of viral infection.[38] Lymphocytes are mainly divided into B and T cells. T lymphocytes are the cells that are programmed to recognize, respond to and remember antigens. Enhancement of T cell activity for prevention or treatment of cancer and viral infection is a central goal in the field of immunology. T cell activation can be achieved through exposure to cytokines such as IL-12 and IL-18.[39, 40] However, this approach has limited success because high toxicity was observed from the systemic administration of these cytokines[41] and the pleotropic effects of these agents. We believe the most useful approach for the prevention of disease and viral infection would be an agent that produces a modest induction of lymphocyte function with relative specificity among immune effector cells, e.g. producing the antiviral cytokines like IFNs. Expression or release of IFN-γ has been reported in activated lymphocytes activated by LPS.[42, 43] Self-activated IFN-γ expression has also been observed

in both mouse peritoneal macrophages and human peripheral blood lymphocytes.[44]

In this study, we found that acteoside, a phenylpropanoid glycoside, which can be isolated from *L. purpurascens*, was able to specifically enhance IFN-γ production in mouse lymphocytes in a dose-dependent manner (Fig.1A). In the present study, we identified that the induced IFN-γ is a new molecular target of viral infection. The supernatant from the acteoside treated group showed an anti-VSV activity in vitro (Fig.7). Also *in vivo*, acteoside-treated mice were protected from being infected with influenza. Mechanistically, we showed that acteoside elevated the expression level of T-bet on T cells, and subsequently activated the IFN-γ promoter. This increases the likelihood that pleiotropic effects on immune activation and systemic toxicity of the agent might be limited.

Our findings provide a new avenue to prevent or treat infectious diseases using natural products through enhancing T cell function. Like many other natural products, acteoside is likely relatively safe when compared to the administration of cytokines as no substantial toxicities were observed in mice treated with up to 800 mg acteoside/kg body weight (data not shown).

Therefore, acteoside may present a new approach to prevent or treat the infection disease.

Acteoside selectively activates T cells through regulating production of IFN-γ. Therefore, *in vivo,* acteoside will most likely achieve its infection prevention or treatment effects through increasing lymphocytes IFN-γ secretion to activate other innate immune components such as macrophages[45] as well as adaptive immune components such as CD8+ T cells.[46,47] Unlike cytokine stimulation, which usually induces both IFN-γ production and cytotoxicity, the selective induction of CD4 and CD8 cell IFN-γ production by acteoside also provides a good opportunity to separate the two major functions of CD3 cells, cytokine production and cytotoxicity, especially when cytotoxicity may cause damage to normal tissues.

Mechanistically, we found that acteoside appeared to stimulate proliferation of lymphocytes, hence leading to the enhancement of IFN-γ production. When compared to the untreated control group, the cell viability of lymphocytes exposed to acteoside (1.25-160 μM) was enhanced in a concentration- and time-dependent manner. The flow cytometric analysis also revealed that no apoptosis of lymphocytes was found upon the treatment of

acteoside. Collectively, we conclude that acetoside did not induce cytotoxicity in vitro.

As far as we can see, the current study is the first to report about the mechanism by which acteoside induced proliferation of mouse lymphocytes. ERK signaling is part of the MAPK superfamily, and is well known for its ability to modulate cell survival in response to external stimuli. Recent studies have suggested a more complicated role of ERK in which its activation could promote cell proliferation in mammalian cells under certain conditions.[48] The antiviral effect of acteoside was plausibly mediated via the phosphorylation of ERK1/2, or the activation of ERK.

Firstly, the activation of ERK1/2 was measured at 24 h after acteoside treatment according to our previous study. Acteoside was found to increase the phosphorylation of ERK1/2. In order to further explore the role of ERK1/2 in the proliferation of acteoside, we applied ERK1/2 inhibitor U0126, the commonly used tool drugs for the detection of ERK signal. In the current study, we found that the proliferation tolerance induced by acteoside was blocked by the inhibitor. Thus, our findings demonstrate that ERK signaling pathway is essential to the proliferation tolerance induced by acteoside pretreatment in lymphocytes.

T-bet is a member of the T-box family of transcription factors that regulates lineage commitment in CD4+ T lymphocytes in part by activating IFN-γ.[49] IFN-γ is known to be produced most prominently by CD8+ T cells, and is vital for the control of microbial pathogens.[49] T-bet is expressed in T cells, which correlates with IFN-γ expression, and T-bet has been reported to trans-activate the IFN-γ gene and induce both endogenous IFN-γ production and chromatin remodeling of individual IFN-γ alleles.[50] In agreement with this finding, our results showed that acteoside treatment simultaneously induced IFN-γ production and T-bet expression in CD4+ and CD8+ T cells (Fig. 3).

Mechanistically, using a luciferase reporter assay, our initial studies clearly indicated that IFN-γ promoter activity can be significantly induced by acteoside in RAW264.7 cells which was consistent with our hypothesis. To increase reliability, we used the microarray for confirmation. Hierarchical cluster analysis showed a close association in gene expressional responses of the T cells causing by acteoside. Figure 6 shows a list of some of the genes identified on arrays to be regulated in common in T cells. The regulation of the genes is also shown for treatments with acteoside. The results clearly show that the gene expression profiles are quite different between acteoside and PBS treatment. The strong upregulation of Jak3, Cd3d, Nr4a1 and Sic2a1 has been

545 linked to interaction with the T cell activation and may contribute to the
546 antiviral state by causing an increase in the levels of IFN-γ. Thus, for acteoside,
547 there is a reasonable agreement between our in vitro observations using
548 microarrays and in vitro or *in vivo* responses.

549 In our study, enrichment of KEGG pathways revealed that the possible
550 pathways involved in the cells treated with acteoside. The Jak-STAT pathway
551 is initiated in response to cytokines, such as interleukins and IFNs, and growth
552 factors. In this study, acteoside was found to be in Jak-STAT signaling,
553 including JAK3, SOCS3 and CISH which are targets of acteoside. This
554 suggests that the Jak-STAT pathway may be affected by acteoside (Table 1).
555 The Cytokine-cytokine receptor interaction has been shown to regulate the
556 expression of cytokine genes involved in the immune response to pathogens.
557 These genes included Fas, IL10, Il2ra, Il21, Ccl3, Tnfsf8 and Ccl4 (Table 1).
558 This demonstrated that acteoside-treated T cell might be involved in the
559 complex signaling pathways.

560 Studies on the *in vitro* and *in vivo* antiviral activity of acteoside are very
561 limited. To our knowledge, the present study describes for the first time the
562 antiviral effects of acteoside on endogenesis of IFN-γ in WISH cells. We found
563 that pre-treatment with IFN-γ induced by acteoside could protect the WISH

cells from VSV infection. It indicates that acteoside-induced IFN-γ production could play a role in reducing viral infection. Furthermore, our *in vivo* study was the first to report the effect of acteoside on pulmonary edema in a viral infectious model. Acteoside at a dose of 80 mg/kg, which was equivalent to the human dose based on its active metabolite exposure, significantly reduced influenza virus–induced lung pathology. The mouse model used here and lung viral load reduction seen in our study are consistent with previous data by the glycosides which contained acteoside.[29] We demonstrate that the beneficial effects in survival and lung pathology observed in the acteoside group can be attributed to the reduction lung inflammatory lesions.

5 Conclusions

In summary, we identified a natural antiviral product, acteoside, which effectively stimulates IFN-γ secretion in T cells. Importantly, acteoside induces IFN-γ expression in lymphocytes at both the translational and transcriptional levels. The current study showed that acteoside treatment induced cell proliferation in mouse lymphocytes. At the molecular level, we observed that acteoside activates T-bet, and subsequently enhances the activity of IFN-γ promoter. Moreover, our study also demonstrated that acteoside treatment

provided anti-VSV effect in vitro and anti-influenza effect *in vivo*. The anti-viral function of acteoside was plausibly mediated through ERK activation and the enhancement of IFN-γ production. To date, acteoside is the best-characterized stimulus for IFN-γ expression. Thus, we propose that acteoside, as an orally antiviral agent, is potentially a prophylactic and/or therapeutic remedy for the management of viral infection in both humans and livestock.

Abbreviations

Interleukin, IL; Interferon, IFN; Tumor Necrosis Factor, TNF; Con A, Concanavalin A; VSV, Vesicular stomatitis virus

Conflict of interest

The author has no conflict of interest.

Acknowledgements

The authors thank Shenzhen Institute of Tsinghua University for providing VSV virus and Institute of Tropical Medicine, Guangzhou University of Chinese Medicine for providing Influenza A Virus H1N1 type (H1N1). This study was supported by grants from the Shenzhen Science and Technology Innovation Committee of China,

602 with grant numbers KQCX20140522111508785, CXZZ20150601110000604 and
603 ZDSYS201506031617582; the National Natural Science Foundation of China with
604 grant number 31500285; the Natural Science Foundation of Guangdong Province with
605 grant number 2015A030310529 and the Health and Medical Research Fund
606 (12132161) of the Food and Health Bureau, Hong Kong S.A.R., China.

607

References

1 B. Pitts, M. A. Hamilton, N. Zelver and P. S. Stewart, *J Microbiol Meth*, 2003, **54**, 269-276.

2 E. Vivier, E. Tomasello, M. Baratin, T. Walzer and S. Ugolini, *Nat. Immunol.*, 2008, **9**, 503-510.

3 S. H. Lee, T. Miyagi and C. A. Biron, *Trends Immunol.*, 2007, **28**, 252-259.

4 F. Novelli and J. L. Casanova, *Cytokine Growth Factor Rev.*, 2004, **15**, 367-377.

5 G. P. Dunn, C. M. Koebel and R. D. Schreiber, *Nat. Rev. Immunol.*, 2006, **6**, 836-848.

6 G. H. Windbichler, H. Hausmaninger, W. Stummvoll, A. H. Graf, C. Kainz, J. Lahodny, U. Denison, E. Muller-Holzner and C. Marth, *Br. J. Cancer*, 2000, **82**, 1138-1144.

7 T. Jahn, M. Zuther, B. Friedrichs, C. Heuser, S. Guhlke, H. Abken and A. A. Hombach, *Plos One*, 2012, **7**.

8 M. Strengell, S. Matikainen, J. Siren, A. Lehtonen, D. Foster, I. Julkunen and T. Sareneva, *J. Immunol.*, 2003, **170**, 5464-5469.

9 K. Wagner, P. Schulz, A. Scholz, B. Wiedenmann and A. Menrad, *Clin. Cancer Res.*, 2008, **14**, 4951-4960.

10 M. R. Baer, S. L. George, M. A. Caligiuri, B. L. Sanford, S. M. Bothun, K. Mrozek, J. E. Kolitz, B. L. Powell, J. O. Moore, R. M. Stone, J. Anastasi, C. D. Bloomfield and R. A. Larson, *J. Clin. Oncol.*, 2008, **26**, 4934-4939.

11 A. Gowda, A. Ramanunni, C. Cheney, D. Rozewski, W. Kindsvogel, A. Lehman, D. Jarjoura, M. Caligiuri, J. C. Byrd and N. Muthusamy, *Mabs-Austin*, 2010, **2**, 35-41.

12 P. G. Fraenkel, S. B. Rutkove, J. K. Matheson, M. Fowkes, M. E. Cannon, M. E. Patti, M. B. Atkins and J. A. Gollob, *J. Immunother.*, 2002, **25**, 373-378.

13 M. L. Salem, W. E. Gillanders, A. N. Kadima, S. El-Naggar, M. P. Rubinstein, M. Demcheva, J. N. Vournakis and D. J. Cole, *J. Interferon Cytokine Res.*, 2006, **26**, 593-608.

14 S. M. Amos, C. P. M. Duong, J. A. Westwood, D. S. Ritchie, R. P. Junghans, P. K. Darcy and M. H. Kershaw, *Blood*, 2011, **118**, 499-509.

15 J. R. Schoenborn and C. B. Wilson, *Adv. Immunol.*, 2007, **96**, 41-101.

16 C. McCaughey, *Ulster Med J*, 2010, **79**, 46-51.

17 N. P. Johnson and J. Mueller, *Bull Hist Med*, 2002, **76**, 105-115.

18 J. K. Taubenberger and D. M. Morens, *Emerging Infect. Dis.*, 2006, **12**, 15-22.

19 J. S. M. Peiris, K. Y. Yuen, A. D. M. E. Osterhaus and K. Stöhr, *N. Engl. J. Med.*, 2003, **349**, 2431-2441.

20 D. M. Morens and A. S. Fauci, *PLoS Pathog.*, 2013, **9**.

21 D. Rajasekaran, E. A. Palombo, T. C. Yeo, D. L. S. Ley, C. L. Tu, F. Malherbe and L. Grollo, *Plos One*, 2013, **8**.

22 X. Y. Wang, W. Jia, A. H. Zhao and X. R. Wang, *Phytother Res*, 2006, **20**, 335-341.

23 N. Uchide and H. Toyoda, *Mini Rev Med Chem*, 2008, **8**, 491-495.

24 U. Grienke, M. Schmidtke, J. Kirchmair, K. Pfarr, P. Wutzler, R. Durrwald, G. Wolber, K. R. Liedl, H. Stuppner and J. M. Rollinger, *J. Med. Chem.*, 2010, **53**, 778-786.

25 M. G. Ison, *Curr Opin Virol*, 2011, **1**, 563-573.

26 S. R. Fauce, B. D. Jamieson, A. C. Chin, R. T. Mitsuyasy, S. T. Parish, H. L. Ng, C. M. R. Kitchen, O. O. Yang, C. B. Harley and R. B. Effros, *J. Immunol.*, 2008, **181**, 7400-7406.

27 D. J. Newman and G. M. Cragg, *J. Nat. Prod.*, 2012, **75**, 311-335.

28. K. U. Bindseil, J. Jakupovic, D. Wolf, J. Lavayre, J. Leboul and D. van der Pyl, *Drug Discov. Today*, 2001, **6**, 840-847.

29 X.P. Hu, M.M. Shao, X. Song, X.L. Wu, L. Qi, K. Zheng, L. Fan, C.H. Liao, C.Y. Li, J. He, Y.Y. Hu, H.Q. Wu, S.H. Li, J. Zhang, F.X. Zhang and Z.D. He, *J Ethnopharmacol*, 2016, **179**, 128-136.

30 R. A. Burgos, K. Seguel, M. Perez, A. Meneses, M. Ortega, M. I. Guarda, A. Loaiza and J. L. Hancke, *Planta Med.*, 2005, **71**, 429-434.

31 A. Kiani, F. J. Garcia-Cozar, I. Habermann, S. Laforsch, T. Aebischer, G. Ehninger and A. Rao, *Blood*, 2001, **98**, 1480-1488.

32 A. I. Saeed, V. Sharov, J. White, J. Li, W. Liang, N. Bhagabati, J. Braisted, M. Klapa, T. Currier, M. Thiagarajan, A. Sturn, M. Snuffin, A. Rezantsev, D. Popov, A. Ryltsov, E. Kostukovich, I. Borisovsky, Z. Liu, A. Vinsavich, V. Trush and J. Quackenbush, *BioTechniques*, 2003, **34**, 374-378.

33 W. P. Dai, G. Li, X. Li, Q. P. Hu, J. X. Liu, F. X. Zhang, Z. R. Su and X. P. Lai, *J Ethnopharmacol*, 2014, **155**, 1575-1582.

34 L. Fan, C. H. Liao, S. G. Li, X. J. Huang, X. P. Hu, X. Song, C. L. Fan, Y. Wang, W. C. Ye, Q. R. Kang, K. Zhen, L. P. Liu, Y. C. Jiang, X. M. Fan, J. Zhang, Y. Li, Y. Zeng and Z. D. He, *Phytochem Lett*, 2015, **13**, 177-181.

35 X. Song, C. Y. Li, Y. Zeng, H. Q. Wu, Z. Huang, J. Zhang, R.S. Hong, X. X. Chen, L.Y. Wang, X.P. Hu, W. W. Su, Y. Li and Z. D. He, *J Ethnopharmacol*, 2012, **144**, 584-591.

36 S. M. Hedrick, I. L. Ch'en and B. N. Alves, *Immunol. Rev.*, 2010, **236**, 41-53.

37 J. H. Yu, M. Wei, Z. Boyd, E. B. Lehmann, R. Trotta, H. Mao, S. J. Liu, B. Becknell, M. S. Jaung, D. Jarjoura, G. Marcucci, L. C. Wu and M. A. Caligiuri, *Eur. J. Immunol.*, 2007, **37**, 2549-2561.

38 J. K. Hwang, J. Y. Chung, N. I. Baek and J. H. Park, *Int. J. Antimicrob. Agents*, 2004, **23**, 377-381.

39 R. V. Luckheeram, R. Zhou, A. D. Verma and B. Xia, *Clin. Dev. Immunol.*, 2012, DOI: Artn 92513510.1155/2012/925135.

40 M. Wolfl and P. D. Greenberg, *Nat Protoc*, 2014, **9**, 950-966.

41 S. A. Rosenberg, M. T. Lotze, J. C. Yang, P. M. Aebersold, W. M. Linehan, C. A. Seipp and D. E. White, *Ann. Surg.*, 1989, **210**, 474-485.

42 D. K. Blanchard, J. Y. Djeu, T. W. Klein, H. Friedman and W. E. Stewart, *J Immunol.*, 1986, **136**, 963-970.

43 T. K. Varma, C. Y. Lin, T. E. Toliver-Kinsky and E. R. Sherwood, *Clin. Diagn. Lab. Immunol.*, 2002, **9**, 530-543.

44 K. J. Hardy and T. Sawada, *J. Exp. Med.*, 1989, **170**, 1021-1026.

45 C. F. Nathan, H. W. Murray, M. E. Wiebe and B. Y. Rubin, *J. Exp. Med.*, 1983, **158**, 670-689.

46 M. Q. Ge, A. W. S. Ho, Y. F. Tang, K. H. S. Wong, B. Y. L. Chua, S. Gasser and D. M. Kemeny, *J Immunol.*, 2012, **189**, 2099-2109.

47 F. J. Kos and E. G. Engleman, *J Immunol.*, 1995, **155**, 578-584.

48 W. Zhang and H. T. Liu, *Cell Res.*, 2002, **12**, 9-18.

49 S. J. Szabo, B. M. Sullivan, C. Stemmann, A. R. Satoskar, B. P. Sleckman and L. H. Glimcher, *Science*, 2002, **295**, 338-342.

50 A. C. Mullen, F. A. High, A. S. Hutchins, H. W. Lee, A. V. Villarino, D. M. Livingston, A. L. Kung, N. Cereb, T. P. Yao, S. Y. Yang and S. L. Reiner, *Science*, 2001, **292**, 1907-1910.

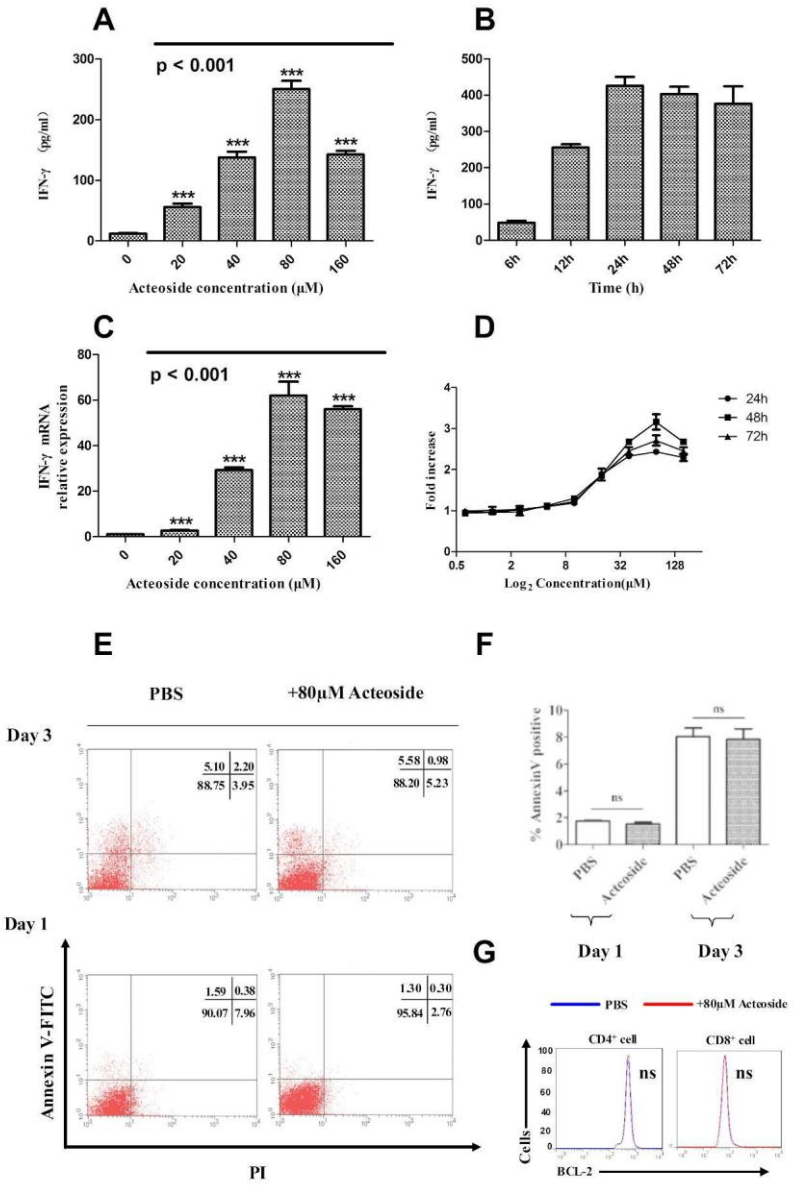

Fig. 1 Stimulatory effect of acteoside on IFN-γ production and cell proliferation in mouse primary lymphocytes. (A) Purified primary mouse lymphocytes (1×106 cells/ml) were treated with different concentrations of acteoside for 48 h and levels of IFN-γ secretion were assessed by ELISA. (B) Lymphocytes were treated with acteoside (80 μM) for 12, 24, 48 or 72 h for a time-course study of IFN-γ secretion. (C) mRNA expression of IFN-γ in primary mouse lymphocytes was determined by means of real-time RT-PCR. (D) The proliferation effect of acteoside was determined by CCK-8 assay. Measurements were taken at 24, 48

and 72 h. In this CCK-8 assay, the highest rate of lymphocyte proliferation was observed at 48 h when incubated with acteoside at 80 μM. (E-G) Effect of acteoside on apoptosis in primary lymphocytes. (E) Flow cytometric analysis of vehicle-treated and acteoside-treated cells stained with annexin V and propidium iodide (PI) was performed 24 and 72 h post treatment. No significant induction of apoptosis (both early and late apoptosis) was observed in the primary lymphocytes treated with acteoside (80 μM). (F) Annexin V- positive cell population was examined 1 day and 3 days after the treatment of acteoside (80 μM). Data are shown as mean ± S.D. and collected from three individual assays (ns means no significant difference). (G) The intracellular levels of BCL-2, a major apoptotic marker, in CD4+ and CD8+ T cells were examined using flow cytometry. Bars represent standard deviation of mean. Data were analyzed using one-way ANOVA followed by Tukey's multiple comparison test ***$p < 0.001$, compared with control. Data are representative of three independent experiments.

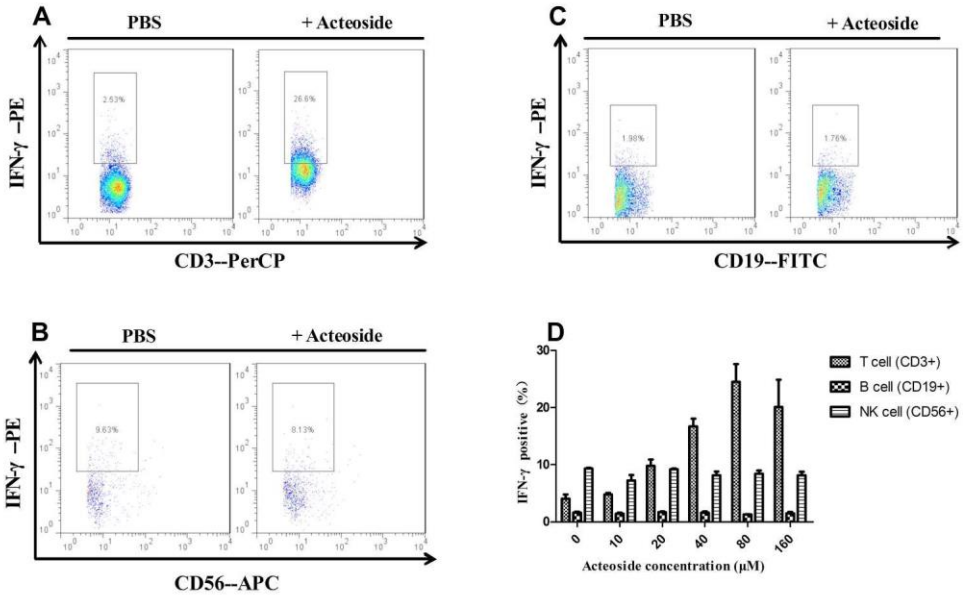

Fig. 2 Effect of acteoside on cytokine production and surface marker expression of mouse IFN-γ-secreting cells. Lymphocytes were stimulated with acteoside for 24 h, fixed and permeabilized using the BD Cytofix/Cytoperm buffer. Cells were co-stained with IFN-γ-PE and fluorescent antibodies: CD3-PerCP (A), CD56-APC (B) and CD19-FITC (C). Supporting Information Figure 2 showed the gating strategy. The fluorescent signals were analyzed using the BD

FACSVerse™ flow cytometer. The differences in the population of IFN-γ-secreting cells among B, NK and T cells were compared using ANOVA (D).

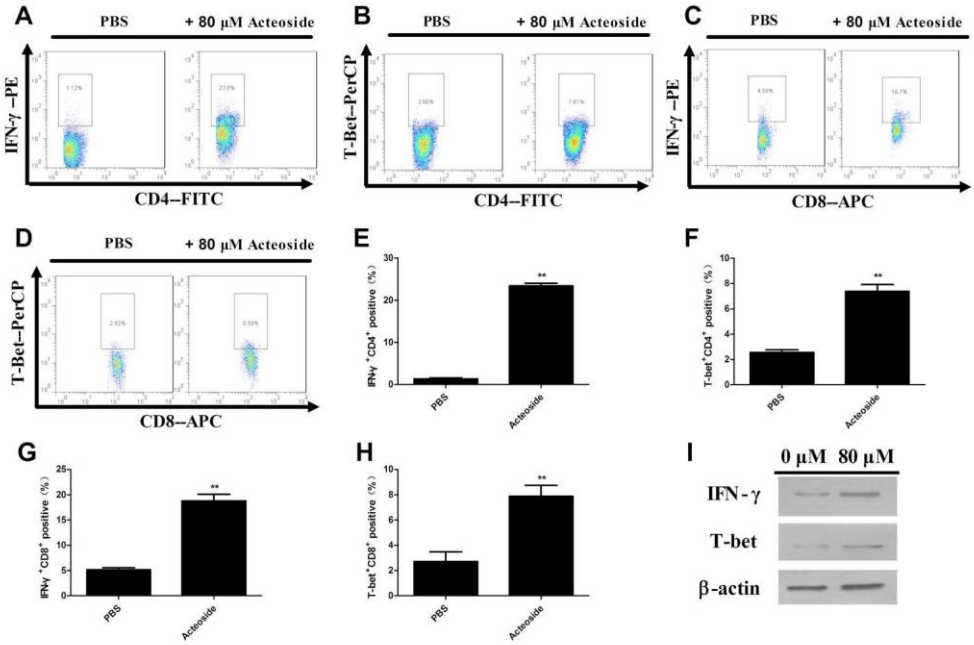

Fig. 3 Effect of acteoside on T-bet and IFN-γ expression in T cells. T-bet and IFN-γ expression in CD4+ T or CD8+ T cells as measured by intracellular staining and flow cytometry of lymphocytes collected from the spleen. Representative dot plots demonstrated the expression levels of IFN-γ (A) and T-bet (B) in acteoside- treated CD4+T cells and IFN-γ (C) and T-bet (D) in acteoside-treated CD8+ T cells. Cumulative histogram showed the percentage of CD4+IFN-γ+ (E), CD4+T-bet+ (F), CD8+IFN-γ+ (G) and CD8+T-bet+ (H) in the primary mouse lymphocytes treated with acteoside (80 μM). (I) Effect of acteoside on protein expression levels of IFN-γ and T-bet. CD3+ T cells were isolated from primary mouse lymphocytes and treated with acteoside at 80 μM for 48 h. Protein levels of IFN-γ and T-bet were examined by means of Western blotting analysis, in which β-actin was served as a loading reference. Error bars denote the S.E.M. *$p < 0.05$ and **$p < 0.01$ (unpaired t-test) ($n = 3$).

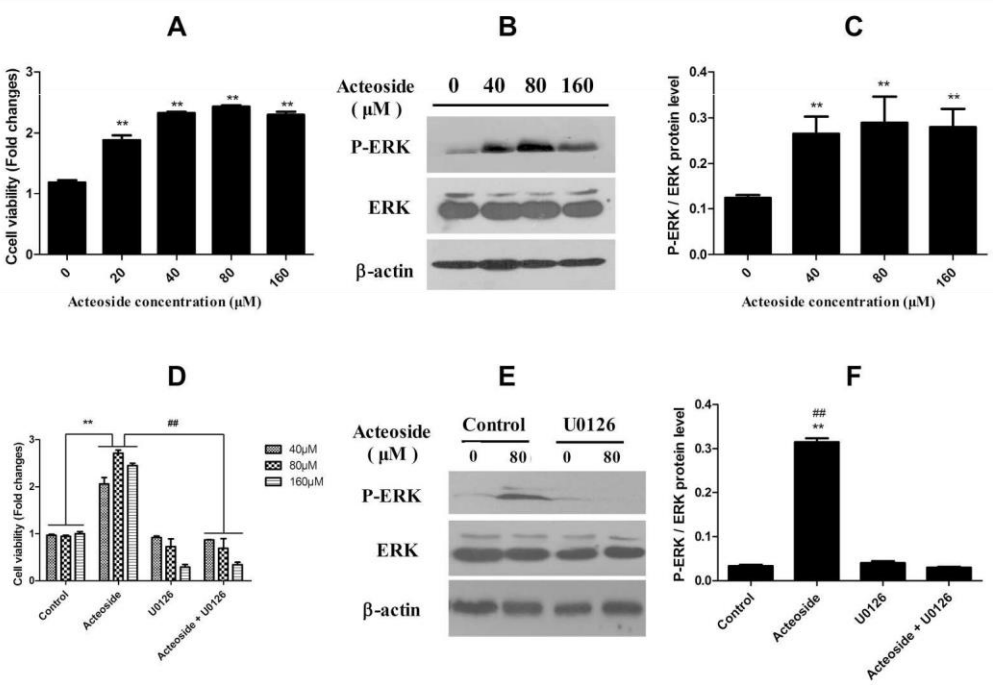

Fig. 4 Effect of acteoside on cell proliferation and ERK expression. (A) Effect of acteoside on proliferation of lymphocytes. Cell viability was measured by CCK-8 assay. The results showed that acteoside promoted cell proliferation in a dose-dependent manner. (B) The effect of acteoside on ERK1/2 activation under different concentration was examined by Western blotting analysis. The level of p-ERK was notably enhanced by acteoside whereas total ERK level was unaffected (C) Band intensities of three representative immunoblotting images were quantified using Bio-rad ImageLab and statistically presented in the graphs. *p<0.05; **p<0.01 when compared to the vehicle control. (D) The stimulatory effect of acteoside on T cell proliferation was abolished by U0126, an ERK1/2 inhibitor. (E) The acteoside-induced ERK phosphorylation was inhibited by U0126. (F) Band intensities of three representative immunoblotting images were quantified using Bio-rad ImageLab and statistically presented in the graphs. **p <0.01 when compared with control; ##p <0.01 when compared with U0126 treatment, n=3.

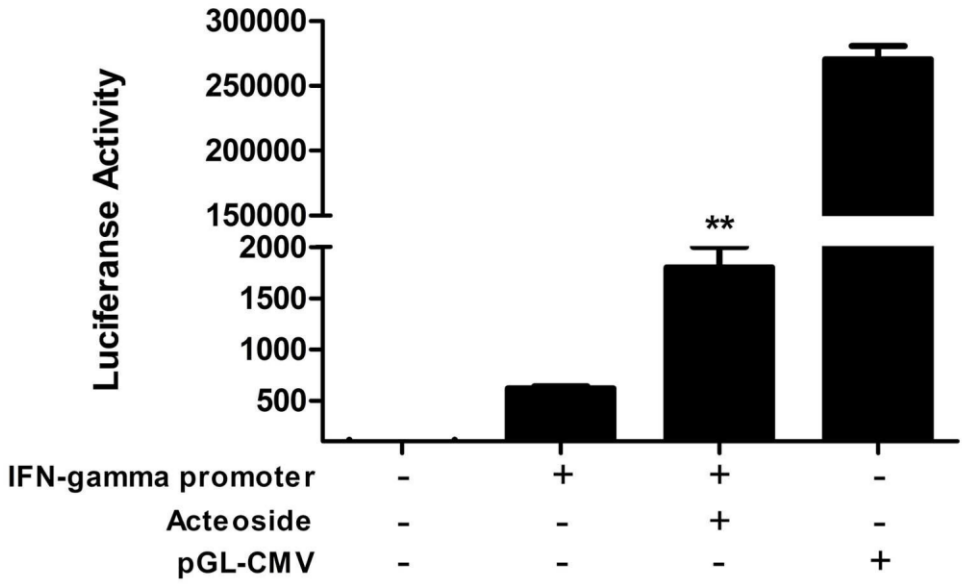

779

780 **Fig. 5** Effect of acteoside on IFN-γ promoter activity. RAW264.7 cells were
781 transfected with either pGL3- IFN-γ promoter or pGL3-basic (empty vector) prior
782 to the exposure of acteoside (80 μM, 24 h). The pGL- CMV Renilla vector was
783 served as a normalizing control. Luciferase activity was correlated to equal
784 amount of total cellular protein for each sample. IFN-γ promoter activity was
785 notably induced (approximately 3-fold) by the acteoside treatment when
786 compared to the control. Data are the representatives of 3 independent
787 experiments. **$p \leq 0.01$ vs. Control.

788

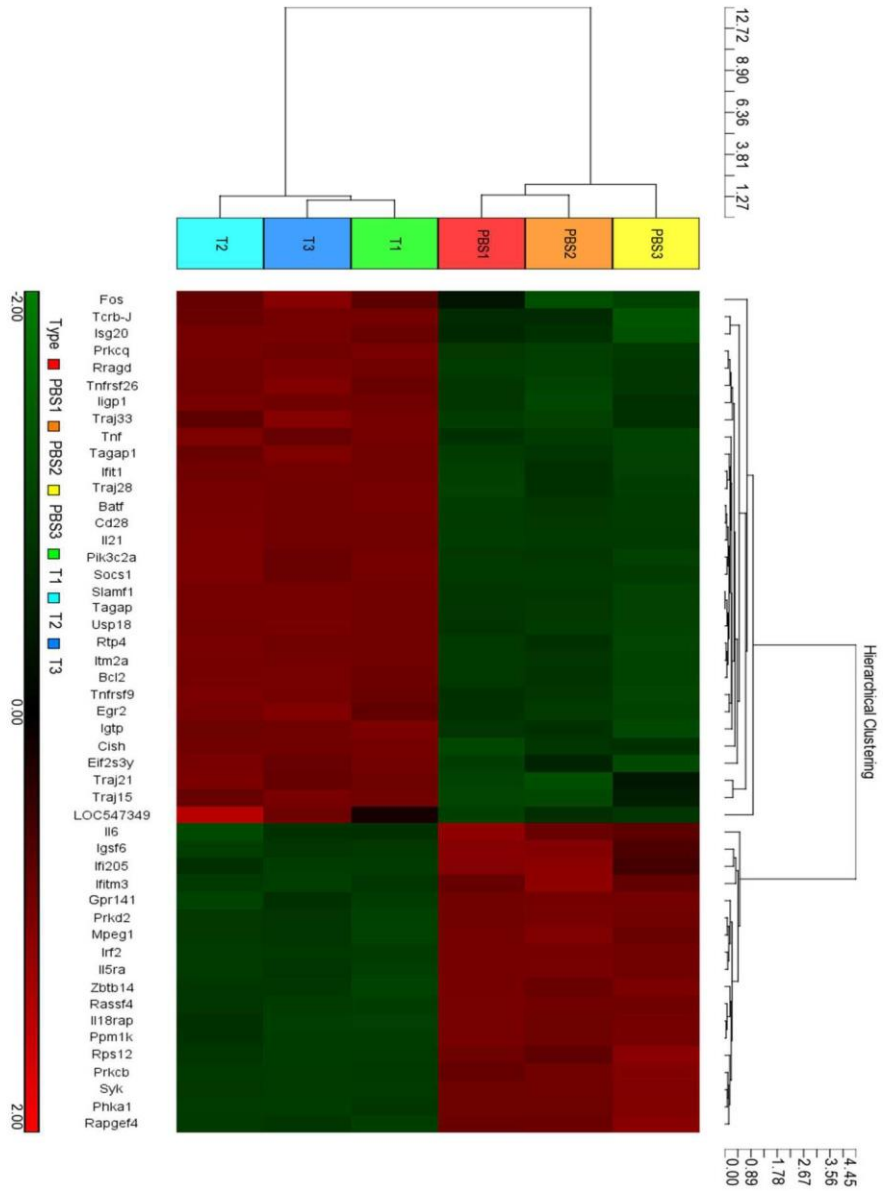

789

790 **Fig. 6** Gene expression profile post acteoside treatment. CD3+ T cells were
791 treated with acteoside (80 μM) for 48 h and RNA was collected as specified in
792 "Microarray hybridization and analysis" for Microarray gene expression analysis.
793 Presented is a heat map of 49 genes with the most dramatic changes upon
794 acteoside treatment.

795

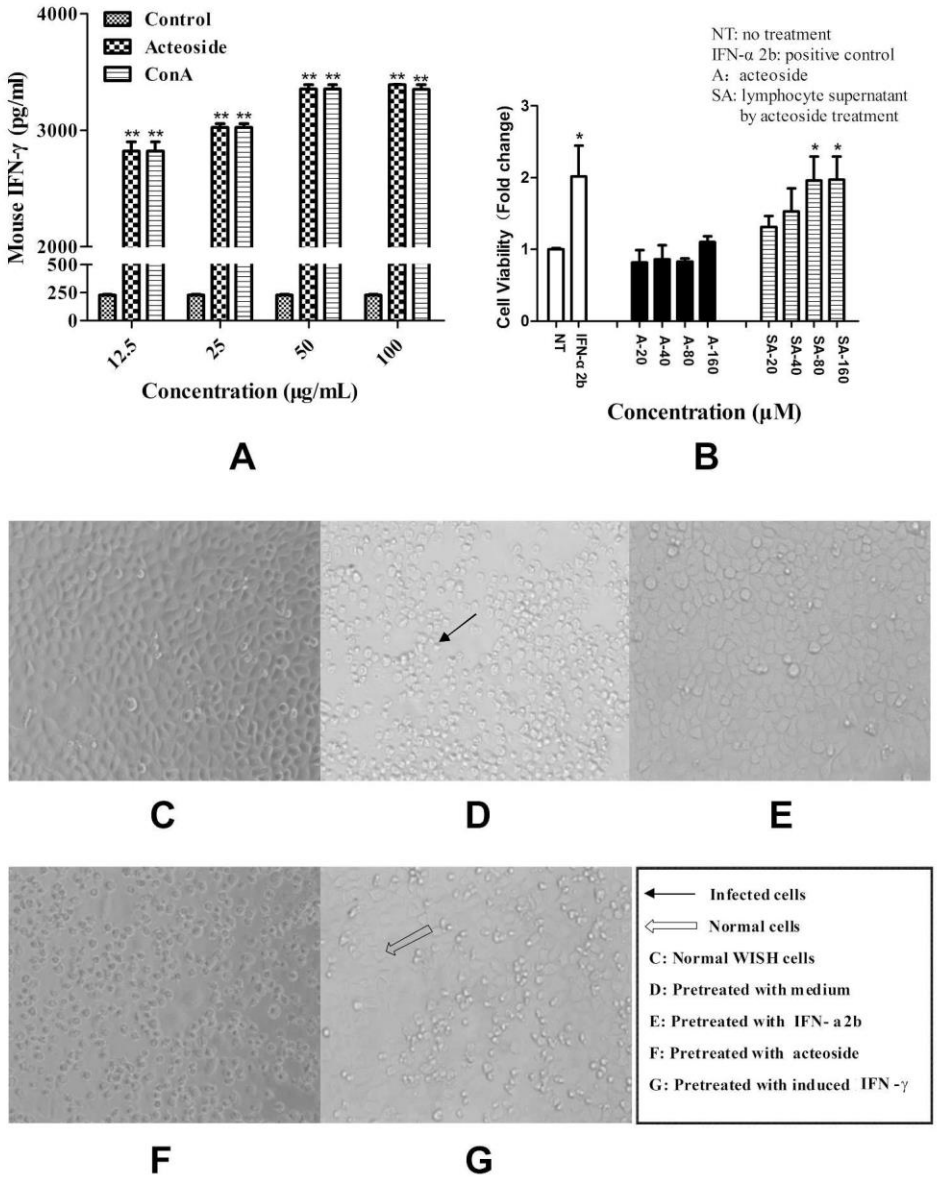

796

797 **Fig. 7** Anti-VSV effects of IFN-γ induced by acteoside. A. Effect of acteoside on
798 IFN-γ in mouse lymphocytes. Purified primary mouse lymphocytes
799 (1×107cells/ml) were treated with different concentrations of acteoside for 48 h.
800 The levels of IFN-γ secretion were assessed by ELISA. ConA was used as a
801 positive control. The supernatants were collected and IFN-γ was measured by
802 ELISA for the anti-VSV experiment. B. Effects of acteoside on VSV-induced cell
803 death. All groups were attacked by VSV after treating with different
804 concentrations of acteoside. Cell viability (%) = OD (Experimental groups or
805 positive group) / OD (viral group). The A group is short for acteoside group. The
806 SA group is the abbreviation of IFN-γ plus acteoside. NT means negative
807 treatment. C-G. Anti-VSV effects of IFN-γ induced by acteoside (100×).
808 Confluent monolayers of WISH cells were exposed to a standard interferon

preparations and the lymphocyte supernatants treated with acteoside. Twenty four hours later, the cells were washed and then treated with VSV (100CCID50) per well. After another continuous culture of 24 h, cell viability was determined by CCK8. (C) Morphology of WISH cells in culture was observed with ×100 magnification on an inverted phase- contrast microscope. Morphology of normal WISH cells; (D) The WISH cells were pretreated with medium and then attacked by VSV; (E) The WISH cells were pretreated with human recombinated IFN-α2b and then attacked by VSV; (F) The WISH cells were pretreated with acteoside and then attacked by VSV; (G) The WISH cells were pretreated with IFN-γ induced by acteoside and then attacked by VSV. Data are calculated using one-way ANOVA. *p<0.05, **p<0.01.

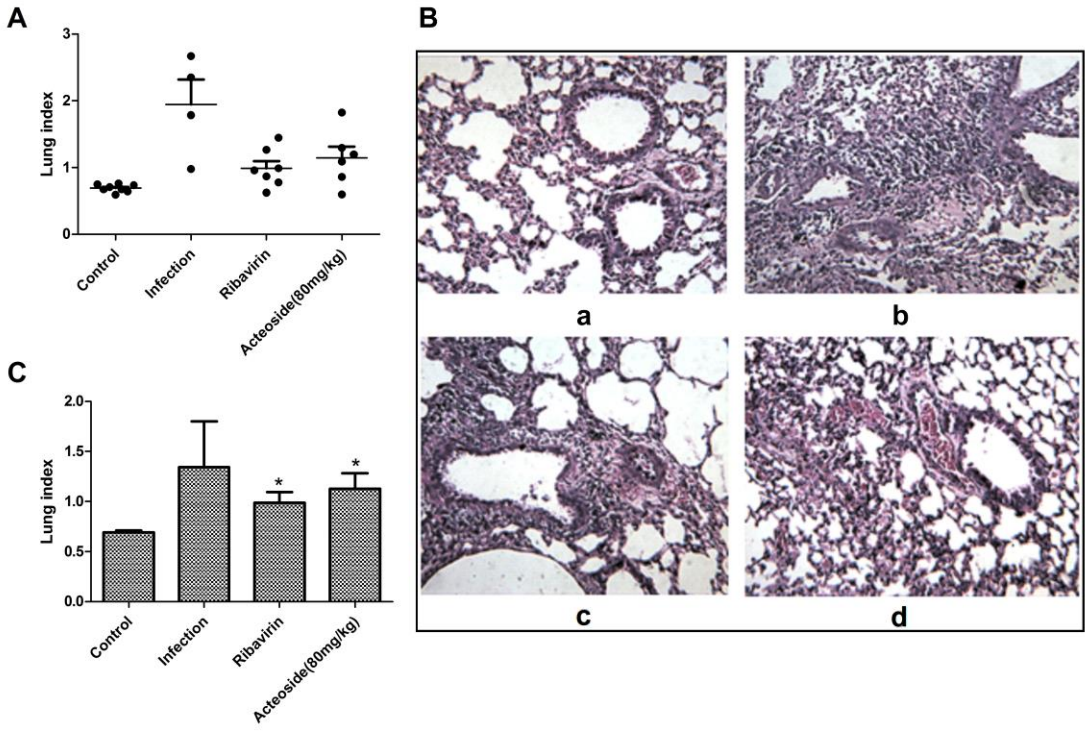

Fig. 8 Antiviral effects by acteoside in vivo. Acteoside treatment decreased the lung weight/body weight ratio and reduced alveolar exudation of H1N1-infected mice. Six-week-old C57BL/6 mice were used. Their lung weight/body weight ratio was determined (A and B), and lung tissues were collected for histopathological examination (H & E stain) (C) at day 8 after the acteoside treatment. The images of histopathological change of lungs from a representative animal in treatment group are shown. Control group lung (a); Infected group lung (b); Ribavirin group lung (c); Acteoside group (80mg/kg) lung (d); The image are represented with magnification of 100×. Data represent means ± S.E.

832 Tables

833

834 **Table 1** Pathway analysis with treatment of acteoside involved in immune
835 response pathway

836

837

838

839 **Table 1** Pathway analysis with treatment of acteoside involved in immune response pathway

Treatment with acteoside	KEGG Pathway	Target genes	*P* value
Up-regulation	mmu04060:Cytokine-cytokine receptor interaction	CCL3, TNF, IL9R, CSF2RB2, IL18, CSF1, CXCL2, IL4RA, BMPR2, CXCL9, PF4, CCL4, IL10, CXCL10, CLCF1, IL10RA, CSF2RB, IL1B, FAS, IL1A, IL6, IL18RAP, TNFSF4, IL2RA, IL21, TNFSF8, CCR8, TNFRSF9, CCR6, PPBP, CXCL13, CCR4, CCR3, CXCL16, CCR2, IL5RA, IL2	1.55518E-10
	mmu04640:Hematopoietic cell lineage	IL6, IL9R, IL2RA, TNF, CD3D, CD3E, CSF1, IL4RA, ITGA1, ITGA2, ITGA4, GP9, CD38, CD55, IL1B, IL5RA, IL1A	7.93341E-07
	mmu04630:Jak-STAT signaling pathway	IL6, IL9R, IL2RA, SOCS3, CSF2RB2, IL4RA, SOCS1, IL21, CISH, IL10, SPRY1, CLCF1, IL10RA, SPRED2, CSF2RB, IL5RA, JAK3, MYC, IL2	0.000154724
	mmu05322:Systemic lupus erythematosus	HIST1H2AB, HIST1H4M, TNF, C3, HIST1H2BG, ELANE, SNRPD1, TRAV7D-3, IL10, C1QB, HIST1H2BN, CD80, HIST1H3A, HIST1H2AI, HIST1H3F, HIST1H4I, CTSG, HIST1H4H	0.000198817
	mmu05332:Graft-versus-host disease	PRF1, IL6, TNF, CD80, IL1B, FAS, TRAV7D-3, KLRD1, KLRC1, IL1A, IL2	0.000233052
	mmu04062:Chemokine signaling pathway	CCL3, VAV3, LYN, HCK, CXCL2, CXCL9, PF4, CCL4, CXCL10, PRKCB, CCR8, CCR6, PPBP, CCR4, CXCL13, CXCL16, CCR3, RASGRP2, CCR2, JAK3	0.0005273
	mmu04210:Apoptosis	PRKAR2B, CASP6, IRAK3, TNF, CSF2RB2, BCL2, IL1B, CSF2RB, FAS, CAPN2, ATM, IL1A	0.001751684
	mmu04650:Natural killer cell mediated cytotoxicity	PRF1, CD244, VAV3, TNF, CD247, KLRK1, NCR1, PRKCB, CD48, PLCG2, ZAP70, FAS, KLRD1, KLRC1	0.003314388
	mmu05020:Prion diseases	EGR1, C1QB, NOTCH1, IL6, IL1B, PRNP, IL1A	0.004374742
	mmu04672:Intestinal immune network for IgA production	ICOSL, IL6, CD80, ITGB7, ITGA4, TRAV7D-3, IL10, IL2	0.010338298
	mmu04621:NOD-like receptor signaling pathway	NLRC4, IL6, TNF, NAIP2, IL18, CXCL2, IL1B, CASP1	0.021160096

	mmu04940:Type I diabetes mellitus	PRF1, TNF, CD80, IL1B, FAS, TRAV7D-3, IL1A, IL2	0.02291764
	mmu04623:Cytosolic DNA-sensing pathway	IL6, IL18, IL1B, CASP1, CCL4, ZBP1, CXCL10	0.036913393
	mmu05330:Allograft rejection	PRF1, TNF, CD80, FAS, TRAV7D-3, IL10, IL2	0.04611816
Down-regulation	mmu04060:Cytokine-cytokine receptor interaction	IL6, IL18RAP, IL9R, CSF2RB2, IL18, CXCL9, PF4, CCR6, PPBP, CXCL13, CLCF1, CXCL16, CCR3, IL10RA, CCR2, IL1B, CSF2RB, IL5RA	0.000239183
	mmu04640:Hematopoietic cell lineage	CD38, CD55, IL6, IL9R, ITGA1, ITGA2, IL1B, IL5RA, ITGA4, GP9	0.000359331
	mmu05322:Systemic lupus erythematosus	HIST1H2AB, HIST1H4M, C3, HIST1H2BG, ELANE, C1QB, HIST1H2BN, CD80, HIST1H3A, HIST1H2AI, HIST1H3F, HIST1H4I, CTSG, HIST1H4H	0.000380479
	mmu04062:Chemokine signaling pathway	CCR6, LYN, PPBP, CXCL13, HCK, CXCL16, CCR3, CCR2, RASGRP2, CXCL9, PF4, PRKCB	0.008999061
	mmu04650:Natural killer cell mediated cytotoxicity	CD48, PRF1, CD244, PLCG2, KLRK1, NCR1, KLRD1, KLRC1, PRKCB	0.015770393
	mmu05332:Graft-versus-host disease	PRF1, IL6, CD80, IL1B, KLRD1, KLRC1	0.018590477
	mmu04621:NOD-like receptor signaling pathway	NLRC4, IL6, NAIP2, IL18, IL1B, CASP1	0.024132676
	mmu04210:Apoptosis	PRKAR2B, IRAK3, CSF2RB2, IL1B, CSF2RB, CAPN2, ATM	0.027994561
	mmu04670:Leukocyte transendothelial migration	VCAM1, CYBB, NCF2, NCF4, PLCG2, RAPGEF4, ITGA4, PRKCB	0.039037746

840

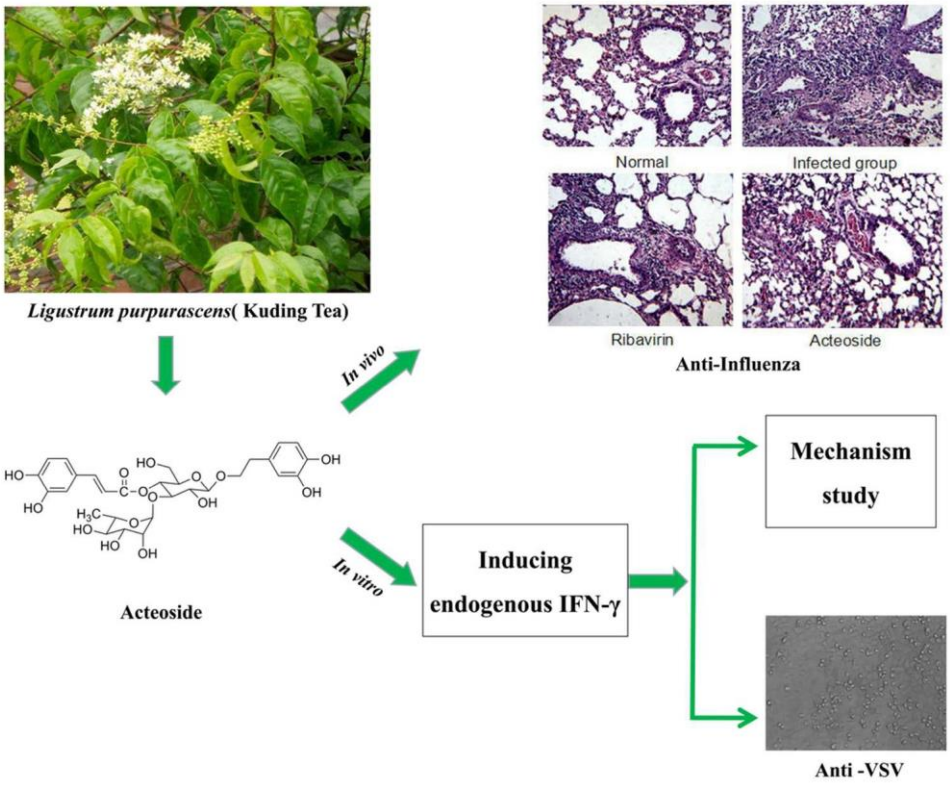
Ligustrum purpurascens(Kuding Tea)
Normal
Infected group
Ribavirin
Acteoside
Anti-Influenza
In vivo
In vitro
Acteoside
Inducing endogenous IFN-γ
Mechanism study
Anti -VSV

841
842
843